Biochimica et Biophysica Acta 1841 (2014) 535–543

Contents lists available at ScienceDirect

Biochimica et Biophysica Acta

journal homepage: www.elsevier.com/locate/bbalip

Bovine lactoferrin binds oleic acid to form an anti-tumor complex similar to HAMLET

Bing Fang [a,b], Ming Zhang [c], Mai Tian [a,d], Lu Jiang [a], Hui Yuan Guo [e], Fa Zheng Ren [a,d,e,*]

[a] Key Laboratory of Functional Dairy, College of Food Science and Nutritional Engineering, China Agricultural University, Beijing 100083, China
[b] Academy of State Administration of Grain, Beijing 100037, China
[c] Beijing Technology and Business University, Beijing 100048, China
[d] Beijing Laboratory for Food Quality and Safety, Beijing 100083, China
[e] Beijing Higher Institution Engineering Research Center of Animal Product, Beijing 100083, China

ARTICLE INFO

Article history:
Received 29 July 2013
Received in revised form 8 December 2013
Accepted 14 December 2013
Available online 22 December 2013

Keywords:
Lactoferrin
Oleic acid
HAMLET
Anti-tumor
Apoptosis
Isothermal titration calorimetry

ABSTRACT

α-Lactalbumin (α-LA) can bind oleic acid (OA) to form HAMLET-like complexes, which exhibited highly selective anti-tumor activity *in vitro* and *in vivo*. Considering the structural similarity to α-LA, we conjectured that lactoferrin (LF) could also bind OA to obtain a complex with anti-tumor activity. In this study, LF–OA was prepared and its activity and structural changes were compared with α-LA–OA. The anti-tumor activity was evaluated by methylene blue assay, while the apoptosis mechanism was analyzed using flow cytometry and Western blot. Structural changes of LF–OA were measured by fluorescence spectroscopy and circular dichroism. The interactions of OA with LF and α-LA were evaluated by isothermal titration calorimetry (ITC). LF–OA was obtained by heat-treatment at pH 8.0 with LD_{50} of 4.88, 4.95 and 4.62 μM for HepG2, HT29, and MCF-7 cells, respectively, all of which were 10 times higher than those of α-LA–OA. Similar to HAMLET, LF–OA induced apoptosis in tumor cells through both death receptor- and mitochondrial-mediated pathways. Exposure of tryptophan residues and the hydrophobic regions as well as the loss of tertiary structure were observed in LF–OA. Besides these similarities, LF showed different secondary structure changes when compared with α-LA, with a decrease of α-helix and β-turn and an increase of β-sheet and random coil. ITC results showed that there was a higher binding number of OA to LF than to α-LA, while both of the proteins interacted with OA through van der Waals forces and hydrogen bonds. This study provides a theoretical basis for further exploration of protein–OA complexes.

1. Introduction

Recently, a complex of α-LA and oleic acid (OA) was identified in human milk [1,2], and was isolated by anion exchange chromatography. The complex was named as HAMLET (human alpha-lactalbumin made lethal to tumor cells) and showed highly selective apoptotic activity against tumor cells both *in vivo* [3,4] and in clinical trials [5,6]. HAMLET specifically referred to the complex prepared by the anion-exchange chromatography column [2,7]; however, this method turned out to be complicated and had a low yield (less than 10 mg each time). Therefore, other simple methods draw the interests of researches [8–12].

α-LA is structurally conserved among species and HAMLET-like complexes can be formed in different species [13,14]. Fragments of bovine α-LA obtained by limited proteolysis can also bind OA and exhibit anti-tumor activity [15]. Furthermore, an equine lysozyme–OA complex was formed by heating at 45 °C [16]. The fatty acid-binding protein, β-lactoglobulin, was also found to form cytotoxic complexes similar to HAMLET [17]. These results all suggested the possibility that HAMLET-like complexes could be formed with other proteins.

Lactoferrin (LF) is a globular, iron-binding protein with a molecular weight of about 80 kDa that is widely represented in various secretory fluids, such as milk, tears, saliva, seminal plasma and nasal secretions [18,19]. The structure of the iron-binding region of LF was similar to that of α-LA [20]. It was reported that the structure of α-LA induced by release of Ca^{2+} favors the binding of OA [21,22]. LF as well as α-LA releases the bound ions at an acidic pH [23] to yield a more open

Abbreviations: α-LA, α-lactalbumin; OA, oleic acid; HAMLET, human alpha-lactalbumin made lethal to tumor cells; LF, lactoferrin; ANS, 1-anilino-8-naphthalenesulfonate; DMEM, Dulbecco's Modified Eagle's Medium; PBS, phosphate buffer solution; PI, propidium iodide; PVDF, polyvinylidene difluoride; PBST, PBS buffer containing 0.05% Tween 20; CD, circular dichroism; ITC, isothermal titration calorimetry; K, binding constant; n, stoichiometry of binding; ΔH, enthalpy change; ΔG, Gibbs free energy change; ΔS, entropy change; LD_{50}, half lethal dose; p-Akt, phosphorylated Akt; p-JNK, phosphorylated JNK; λ_{max}, the maximum emission wavelength of the fluorescence spectrum; Trp, tryptophan

* Corresponding author at: College of Food Science & Nutritional Engineering, China Agricultural University, P.O. Box 287, No. 17 Qinghua East Road, Haidian, Beijing 100083, China. Tel./fax: +86 10 62736344.
E-mail address: renfazheng@263.net (F.Z. Ren).

http://dx.doi.org/10.1016/j.bbalip.2013.12.008
1388-1981/

structure [24,25]. In addition, heat-induced changes of LF also showed some similarity to those of α-LA, resulting in the cleavage of intramolecular disulfide bridges and the exposure of free reactive thiol groups [24].

Although HAMLET-like complexes have been obtained, the binding mechanism remains unclear. The study of other possible protein complexes with OA may benefit the exploration of the binding mechanism of protein and OA. In this study, a LF–OA complex was prepared by a heat-treatment method. The anti-tumor activity, structural changes and apoptosis mechanism were analyzed. These results provide a theoretical basis for further investigation and clarification of the binding site of OA and the development of similar anti-tumor complexes.

2. Materials and methods

2.1. Materials

Bovine LF (85% purity), bovine α-LA (85% purity, Ca^{2+}-free), OA (C18:1:9 cis, ≥99.0% purity, cell culture tested) and 1-anilino-8-naphthalenesulfonate (ANS) were obtained from Sigma (Sigma-Aldrich Chemical Co., St. Louis, MO, USA). Dulbecco's Modified Eagle's Medium (DMEM) containing a high level of glucose, RPMI-1640, fetal calf serum, HEPES buffer solution, penicillin and streptomycin was purchased from Gibco (Life Technologies, USA). All the other chemicals used were of analytical grade.

2.2. Preparation of protein–OA complexes

LF and α-LA were dissolved in phosphate buffer solution (PBS, 10 mM, pH 8.0) to a final concentration of 120 μM. OA was directly added into the protein solution at 50 molar equivalents (OA:protein). The mixtures were then incubated at 45 °C in a water bath for 20 min after vortexing for 30 s. Excess fatty acid in the complexes was removed by centrifugation at 4 °C followed by ultrafiltration using a 3000 kDa cut-off membrane (Sartorius). The LF solution was treated as above but without OA acting as the control LF. PBS prepared at the same volume as the LF solution was subjected to the same procedure and acted as the control buffer.

2.3. Cell lines and cell cultures

Human hepatoma cells (HepG2), human colon tumor cells (HT29) and human breast cancer cells (MCF-7) were from the ATCC. All cells were maintained in media supplemented with 10% fetal bovine serum, 20 U/ml penicillin, 20 μg/ml streptomycin and 10 mM HEPES at 37 °C in an atmosphere of 5% CO_2. For HepG2 and HT29 cells, the media was DMEM while for MCF-7 cells, it was RPMI-1640.

2.4. Oleic acid measurements

The amount of OA in LF–OA and α-LA–OA was quantified using the Free Fatty Acid Quantification kit (BioVision, Mountain View, USA) according to the manufacturer's instructions. Briefly, samples were added to a 96-well plate at several dilutions and known amounts of OA samples were prepared as a standard curve. Fatty acid assay buffer was added to each well to a final volume of 50 μL. 2 μL Acyl CoA synthetase was then added, followed by incubation at 37 °C for 30 min. A solution of enzymes, enhancer and a fatty acid probe was added to each well. After 30 min of incubation at 37 °C in the dark, the absorbance was detected at 570 nm.

2.5. Cell viability assays

Cells were seeded in 96-well plates (Corning, USA) at a density of 1×10^4 cells/well and grown for 24 h. The medium was then removed, and different concentrations of LF–OA, α-LA–OA and OA were added into a new medium without FBS. FBS was added into each well at a final concentration of 10% after 30 min. After 24 h of incubation at 37 °C, cell viability was tested by methylene blue assay according to Felice et al. [26]. The control LF and the control solution were also added to cells at the same volume.

2.6. Apoptosis assay measured by flow cytometry

Cells were seeded into 12-well plates (Corning, USA) at a density of 1×10^5 cells/well and grown for 24 h. LF–OA was added to the wells at a final concentration of 6 μM, while α-LA–OA was added at a final concentration of 60 μM. After 30 min, FBS was added and the cells were incubated for another 24 h. For apoptosis assays, cells were analyzed by flow cytometry using the Annexin V-FITC/propidium iodide (PI) double staining apoptosis detection kit (eBioscience, Mountain View, CA, USA) [12]. Cells were gated by dot plots and for each sample, at least 15,000 cells were analyzed using a FACSCalibur instrument equipped with FACStation running FACSCalibur software (BD Biosciences, San Diego, CA, USA). Each experiment was performed in triplicate.

2.7. Western blot

HepG2 cells were seeded into a 6-well plate (Corning, USA) at a density of 1×10^6 cells/well and grown for 24 h. LF–OA and the control LF were added to the wells at a final concentration of 6 μM. 100 μM OA was used as it caused similar apoptosis activity as LF–OA. After 0.5 h, FBS was added and cells were incubated for another 24 h. Cells treated with control solution served as the control. Cells were then lysed in 100 μL of RIPA lysis buffer (CST) containing 1 mM PMSF for 10 min on ice and then centrifuged at 14,000 *g* for 20 min at 4 °C. The protein content was measured using a BCA protein assay kit (Pierce, USA). The lysates containing 20 μg of protein were separated on 10% SDS-PAGE gels and then electrotransferred onto polyvinylidene difluoride (PVDF) membranes (Millipore, Temecula, CA, USA) with transfer buffer (25 mM Tris, 250 mM glycine and 20% methanol) at 200 mA for 120 min. The membranes were blocked in 5% skim milk powder in PBS buffer containing 0.05% Tween 20 (PBST) for 2 h at room temperature and immunoblotted with primary antibody overnight at 4 °C. After washing with PBST, the membranes were incubated with horseradish peroxidase-conjugated secondary antibody in PBST containing 5% skim milk powder for 1 h at room temperature. After the same washing steps, the blots were developed using an Immobilon Western Chemiluminescent HRP Substrate kit (Millipore) and exposed to X-ray film [27,28].

2.8. Fluorescence spectroscopy

The intrinsic fluorescence spectra were measured at room temperature using a RF-5301PC spectrofluorometer (Shimadzu, Kyoto, Japan). The emission spectra were collected between 300 and 500 nm with an excitation wavelength of 292 nm and a scan interval of 0.2 nm. The slit widths for excitation and emission were set at 3 nm. All experiments were repeated three times. The protein solutions were diluted with the corresponding buffer to a final concentration of 30 μM.

For the ANS-binding measurements, each protein sample was incubated with 50-fold ANS for 15 min at room temperature in the dark. The emission spectrum of ANS was recorded between 400 and 600 nm at a scan interval of 0.2 nm with an excitation wavelength of 390 nm. The emission fluorescence intensities of ANS were also measured to exclude the influence of unbound ANS. The slit widths of excitation and emission were set at 3 nm. The protein concentration for all measurements was 30 μM. All experiments were repeated three times.

2.9. Circular dichroism spectroscopy

Far-UV and near-UV circular dichroism (CD) spectra were measured using a J-810 instrument (Jasco Corporation, Tokyo, Japan) between 200–240 nm and 250–320 nm, respectively. A 1-mm path-length was used. The scan rate was 50 nm per min with an interval of 0.5 nm and the response time was set as 8 s. Each spectrum was averaged from three scans. Baseline spectra were recorded for the buffer and subtracted from the sample. The protein concentration was 30 μM for all measurements. The secondary structure was calculated using the CD Pro software package. All experiments were repeated three times.

2.10. Binding dynamics measured by isothermal titration calorimetry

The binding dynamics of OA to LF and α-LA were carried out at pH 8.0 (10 mM PBS) and 45 °C using an isothermal titration calorimeter (ITC, Nano Series, TA Corporation, USA). LF and α-LA were dissolved in PBS (10 mM, pH 8.0) to the final concentration of 6.41 μM and 11.2 μM, respectively. The titrated OA solution was first dissolved in the alcohol to a concentration of 100 mM and then diluted 100 times by PBS. 190 μL protein solutions were injected into the sample cell and an automated sequence of 23 injections, each adding 2 μL OA solution into the protein solutions spaced at 200 s intervals to allow complete equilibration, was performed. The stirring rate was set at 150 rpm per min. The data were collected automatically and the binding constant (K), stoichiometry of binding (n), standard enthalpy change (ΔH), standard Gibbs free energy change (ΔG) and standard entropy change (ΔS) were analyzed using Launch NanoAnalyze 2.0 software (TA Corporation).

2.11. Statistical tests

Data are presented as mean values ± SD of three independent experiments. Statistical analysis was performed using one-way ANOVA followed by the Student's t test and Duncan's test.

3. Results

3.1. Anti-tumor activity measured by methylene blue assay

The cell viability of tumor cells after treatment with LF–OA, α-LA–LA and OA for 24 h was measured. As shown in Fig. 1a and b, both LF–OA and α-LA–OA exhibited dose-dependent anti-tumor activity. The half lethal doses (LD_{50}) for LF–OA were 4.88, 4.95 and 4.62 μM for HepG2, HT29, and MCF-7 cells, respectively, whereas the LD_{50} of α-LA–OA were 50.18, 45.77 and 47.60 μM for HepG2, HT29 and MCF-7 cells. No anti-tumor activity was observed for the control LF and control buffer at the same concentrations as the complexes (data not shown).

The anti-tumor activity of OA is shown in Fig. 2, where the LD_{50} values of OA were 100.31, 92.40 and 96.46 μM for HepG2, HT29 and MCF-7 cells, respectively. The molecular ratio of OA in LF–OA and α-LA–LA under the preparation condition was 4 and 1, respectively, as quantified by the Free Fatty Acid Quantification kit. At the concentration of the LD_{50} of LF–OA and α-LA–OA, the actual amount of OA was 19.27 and 47.85 μM (mean value of the three cells), respectively. According to the cytotoxicity curves of OA in Fig. 2, cell viability at these concentrations was 101% and 84% (mean value), respectively.

3.2. Apoptosis rate induced by LF–OA and LA–OA measured by flow cytometry

Further confirmation of the anti-tumor activity of LF–OA and α-LA–OA was obtained using an Annexin V-FITC/PI double staining kit (Fig. 3). At 6 μM, LF–OA induced apoptosis in 34.38% (HepG2, Fig. 3a), 32.75% (HT29, Fig. 3b) and 35.08% (MCF-7, Fig. 3c) of the total cells. At 60 μM α-LA–OA, the percentages of apoptotic cells of HepG2 (Fig. 3d), HT29 (Fig. 3e) and MCF-7 (Fig. 3f) were 30.45%, 29.81% and 30.96%, respectively. Almost no apoptotic cells were detected when treated with control LF and control buffer.

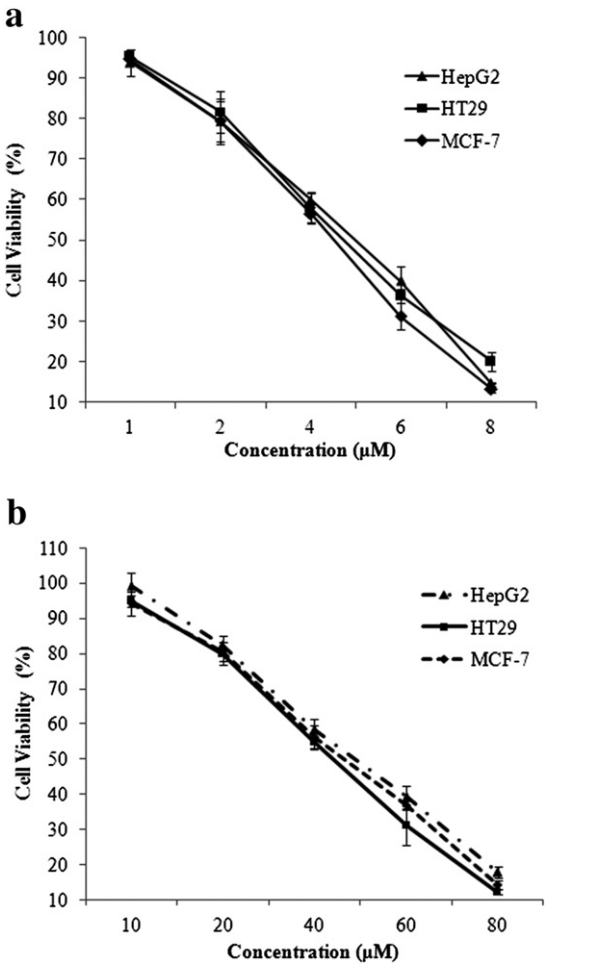

Fig. 1. Cell viability after 24 h of treatment with different concentrations of LF–OA and α-LA–OA as measured by the methylene blue assay. HepG2 (triangle), HT29 (square) and MCF-7 (diamond) cells were treated by 1, 2, 4, 6 and 8 μM LF–OA complexes (a); 10, 20, 40, 60 and 80 μM α-LA–OA complexes (b). The data with error bars are expressed as mean ± s.d. (n = 3).

3.3. Apoptosis pathways analyzed by Western blot

The expression of apoptosis-related proteins after treatment with OA, LF–OA and control LF were analyzed by Western blot (Fig. 4). We first measured the expression of cleaved caspase-3, which belongs to the effector caspase family and directly induces apoptosis. As shown, a dominant band with an apparent molecular weight of 17 kDa for cleaved caspase-3 was detected for all treatment groups when compared with control cells.

To examine the pathway of the apoptosis mechanism, proteins involved in the regulation of mitochondria-mediated and death receptor-mediated apoptosis pathways were then measured. In the mitochondria-mediated pathway, Bax, Bcl-2 and caspase-9 are the primary regulators. As shown in Fig. 4, dominant bands with apparent molecular weights of 21, 25 and 47 kDa for Bax, Bcl-2 and the intact caspase-9, respectively, were detected. Cells treated with OA and LF–OA both showed a higher level of pro-apoptotic Bax accompanied by a lower level of anti-apoptotic Bcl-2, indicating a higher Bax/Bcl-2 ratio. On the contrary, cells treated with control LF showed higher levels of both Bax and Bcl-2, resulting in a lower Bax/Bcl-2 ratio that was similar to control cells. A higher Bax/Bcl-2 ratio leads to the release of

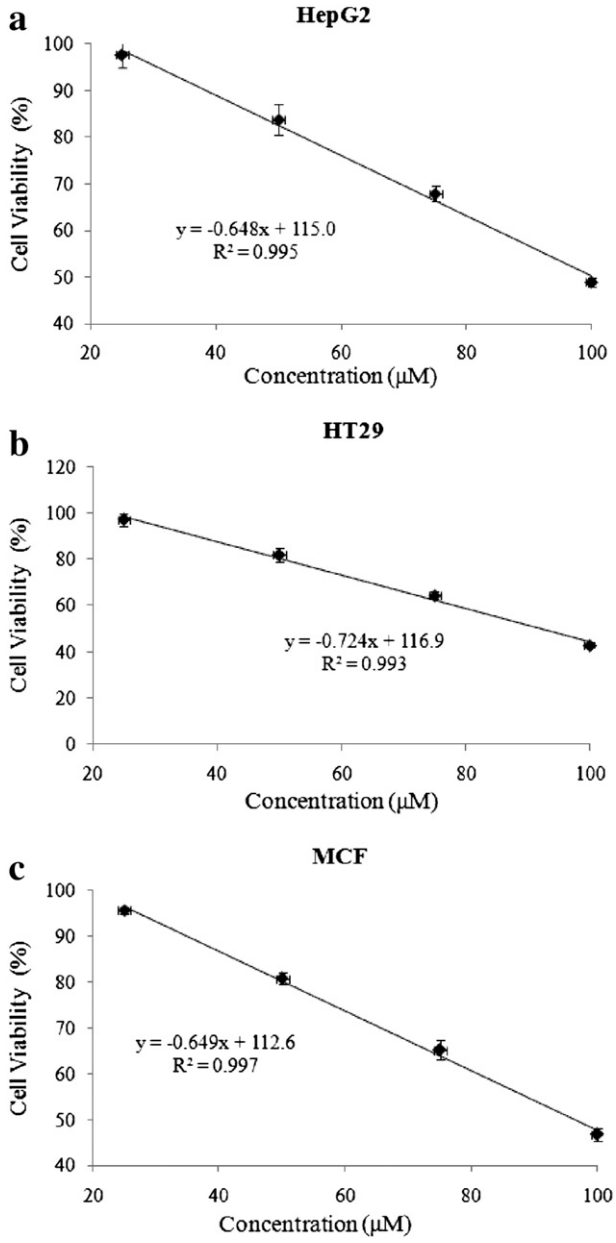

Fig. 2. Cell viability of HepG2 (a), HT29 (b) and MCF-7 (c) cells after 24 h of treatment with 25, 50, 75 and 100 μM OA as measured by the methylene blue assay. The data with error bars are expressed as mean ± s.d. (n = 3).

cytochrome c from mitochondria, which binds and then activates caspase-9 in the cytoplasm. Analysis of the intact caspase-9 suggested that there was more cleaved caspase-9 in cells treated with OA, LF–OA and control LF compared with control cells. Akt participates in the mitochondria-mediated apoptosis pathway and promotes cell survival. Expression of phosphorylated Akt (p-Akt) was decreased in cells treated with OA and LF–OA while activated in cells treated with control LF. This result combined with the lower Bax/Bcl-2 ratio favored the idea that no anti-tumor and apoptosis activity had been observed in cells treated with control LF.

In the death receptor-mediated apoptosis pathway, caspase-8, the initial caspase, was activated in cells treated with OA, LF–OA and control LF. There were light bands at 57 kDa for intact caspase-8 compared with the control cells (Fig. 4). The death-receptor pathway also activates JNK. This in turn activates Bax, which is involved in the mitochondria pathway. Cells treated with OA, LF–OA and control LF all showed increased expression of phosphorylated JNK (p-JNK) compared with the control cells. Although LF–OA and control LF shared some similarities in terms of the expression of proteins that regulate the apoptosis pathways, when the similar cell viability results for LF–OA and OA were taken into account, the apoptosis mechanism of LF–OA was more relevant to that of OA.

3.4. Structural characteristics of LF–OA

The exposure of hydrophobic amino acids (Fig. 5a and b) and hydrophobic regions (Fig. 5c and d) of LF and α-LA induced by binding of OA was analyzed by fluorescence spectroscopy. As shown in Fig. 5a, control LF had an intrinsic fluorescence emission maximum (λ_{max}) at about 332.4 nm while the λ_{max} of LF–OA was significantly red-shifted to 337.4 nm. There was also a significant red-shift when α-LA binds OA (Fig. 5b, from 331.2 nm to 337.6 nm). The red-shift of λ_{max} suggested that tryptophan (Trp) residues were exposed to the solvent. In Fig. 5c, a remarkable increase in ANS fluorescence intensity together with a pronounced blue shift of λ_{max} took place when LF binds OA. Similar changes could also be observed for α-LA–OA, but were less remarkable (Fig. 5d). These results indicated increasing exposure of hydrophobic regions upon binding of OA.

Far-UV and near-UV CD spectroscopy was used to compare the secondary and tertiary structures of LF and α-LA induced by binding of OA (Fig. 6). As shown in Fig. 6A, the near-UV CD spectra of LF–OA showed lower signal intensities compared with the control LF. α-LA also exhibited this phenomenon when binding OA (Fig. 6B). The secondary structure of LF and α-LA with or without OA was calculated from the far-UV CD spectra according to Yang's reference (Table 1). LF–OA showed a decrease of α-helix and β-turn structure compared with the control LF, which turned into β-sheet and random coil ($p < 0.05$). Secondary structure changes of α-LA indicated apparent differences from LF. α-LA had a lower content of β-turn and higher contents of β-sheet and random coil accompanied by an unchanged α-helix content after binding OA. A significant increase of random coil was observed for both α-LA and LF, which indicated the loss of ordered structure after binding with OA.

3.5. Binding dynamics of OA measured by ITC

The binding dynamics of OA to LF and α-LA were monitored by ITC (Fig. 7). The upper figures show the raw calorimetric data and in all cases, the raw ITC data showed exothermic peaks (upward). As the titration progressed, the exothermic peaks decreased until heat values of dilution corresponding to the protein in the buffer alone were reached. The lower figures show a plot of the total heat generated per injection as a function of the molar ratio of OA to protein. All binding isotherms were fit to an independent binding site model and the thermodynamic parameters were obtained (Table 2). The heat of dilution of free OA has been subtracted from this data. The value of K indicates the binding affinity of the interaction. The Ks of OA to LF and α-LA were 1.58×10^5 and 2.09×10^5 M^{-1}, respectively, indicating that OA had almost the same binding strength to both proteins. The values of n, the number of OA-binding sites, for LF and α-LA under the measured condition were 34 and 18, respectively, indicating there were more binding sites in LF than in α-LA.

Besides the binding kinetics, ITC also measured the thermodynamic constants during the binding reaction [29–33]. The Gibbs free energy change, ΔG, which is derived from K, was not significantly different between LF and α-LA. The negative value of ΔG is indicative of spontaneous binding of OA to the proteins [34–38]. Furthermore, this exothermic binding process is accompanied by negative ΔH and ΔS values in the cases of both LF and α-LA (Table 2). The negative ΔH and ΔS changes indicate the importance of van der Waals forces as well as hydrogen bond formation during the titration of OA [34,35,39].

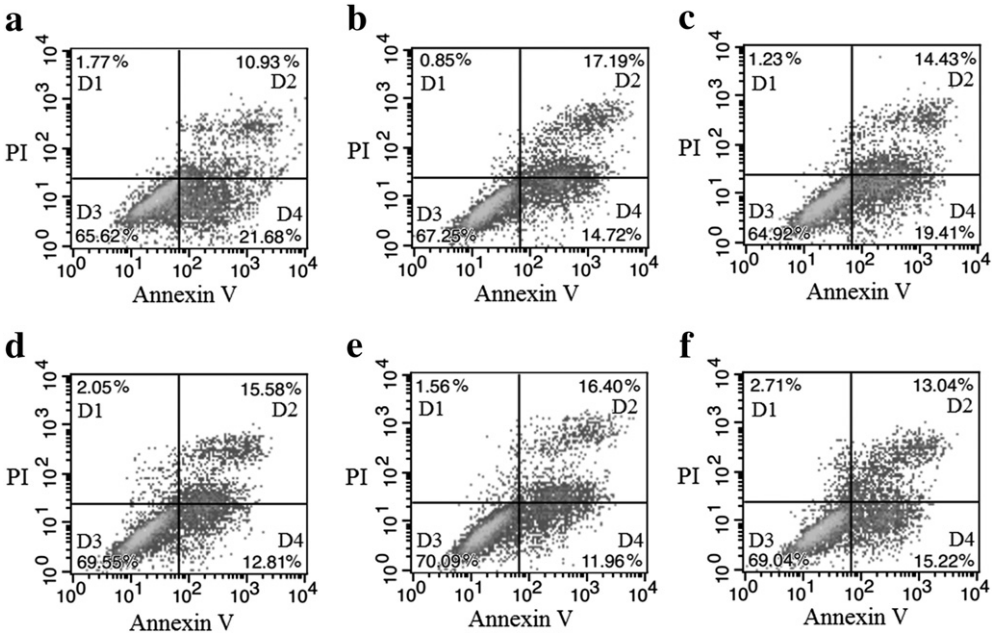

Fig. 3. Apoptosis induced by LF–OA and α-LA–OA in tumor cells analyzed by flow cytometry using an Annexin V-FITC/PI apoptosis testing kit. HepG2 (a and d), HT29 (b and e) and MCF-7 (c and f) were exposed to 6 μM LF–OA (a–c) or 60 μM α-LA–OA (d–f) for 24 h. Early apoptotic cells only bound to annexin V (the lower right D4 region), necrotic or late apoptotic cells bound to both annexin V and PI (the upper right D2 region), while viable cells did not bind to either annexin V or PI (the lower left quadrant D3 region). The upper left D1 region corresponds to cells damaged during the preparation of the cell suspension. The apoptosis rate was calculated after subtracting the value of D1.

4. Discussion

LF as well as α-LA could bind OA to kill tumor cells. The LD_{50} of LF–OA was about 10 times lower than that of α-LA–OA, indicating a much higher anti-tumor activity. OA was found to induce the same degree and type of cell death as HAMLET at the equivalent dose [40]. Meanwhile, our previous study also found that the anti-tumor activity of the complexes increased as the amount of OA bound to α-LA increased [12]. However, according to the results from the Free Fatty Acid Quantification kit, the content of OA in LF–OA was actually lower than that in α-LA–OA at the LD_{50} concentration. Therefore, the higher anti-tumor activity of LF–OA was not because there was a higher concentration of OA in the complex, but indicated the protein also played an important role. α-LA–OA was reported to interact with the tumor cell membrane, enter into cells and localize at the nucleus. Many studies have shown that there is high expression of LF receptors on tumor membranes [41–47], which may favor LF–OA binding to tumor cells and facilitate subsequent interactions with the membrane. In addition, fatty acids with an unsaturated C18 alkyl chain, such as OA, were reported to be a popular enhancer in the delivery of a variety of drugs [48]. It can be inferred that the structure of LF–OA was changed when it interacts with the cell membrane, leading to the exposure of OA, which destroys the selective permeation function of the cell membrane.

LF–OA induced tumor cell apoptosis (Fig. 4), which was similar to the anti-tumor mechanism of HAMLET-like complexes [2,7]. Treatment with LF–OA leads to the outward translocation of phosphatidyl serine, one of the classic characteristics of apoptosis [49,50]. OA also exhibited this phenomenon of apoptosis while the control LF did not (data not shown). Cleaving of caspase-3 can directly lead to apoptosis, which can be activated through both the intrinsic (mitochondrial) and the extrinsic (death-receptor) apoptosis pathways [51,52]. Western blot results suggested that the pro-apoptotic mechanism of LF–OA was attributed to the presence of OA, which is consistent with the results from other studies [40,53–58]. Additionally, the control LF also shares some similarity in its regulation of apoptosis-related proteins with LF–OA. However, there were also pro-survival pathways, such as the higher expression of Bcl-2 and activation of Akt to counteract the apoptosis activity. It can be deduced that LF–OA induced apoptosis through

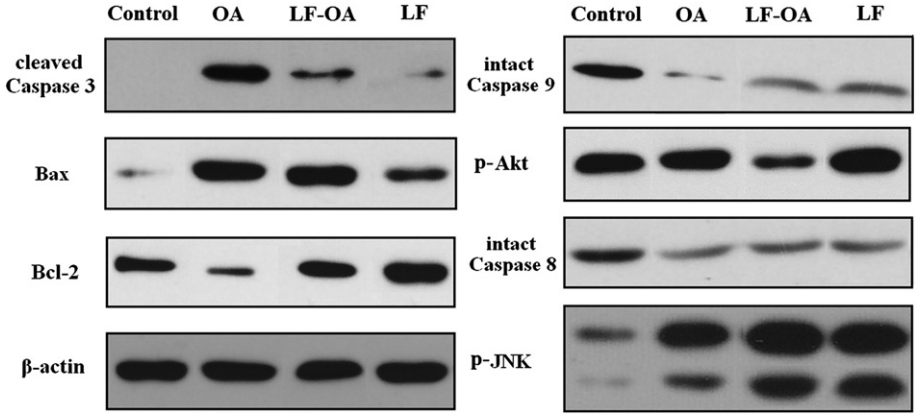

Fig. 4. Expression of cleaved caspase-3, Bax, Bcl-2, intact caspase-9, p-Akt, intact caspase-8 and p-JNK analyzed by Western blot. HepG2 cells were treated with 100 μM OA, 6 μM LF–OA and LF for 24 h. Cells treated with only the medium served as the control. The total cell lysate (20 μg) was subjected to immunoblot analysis using specific antibodies.

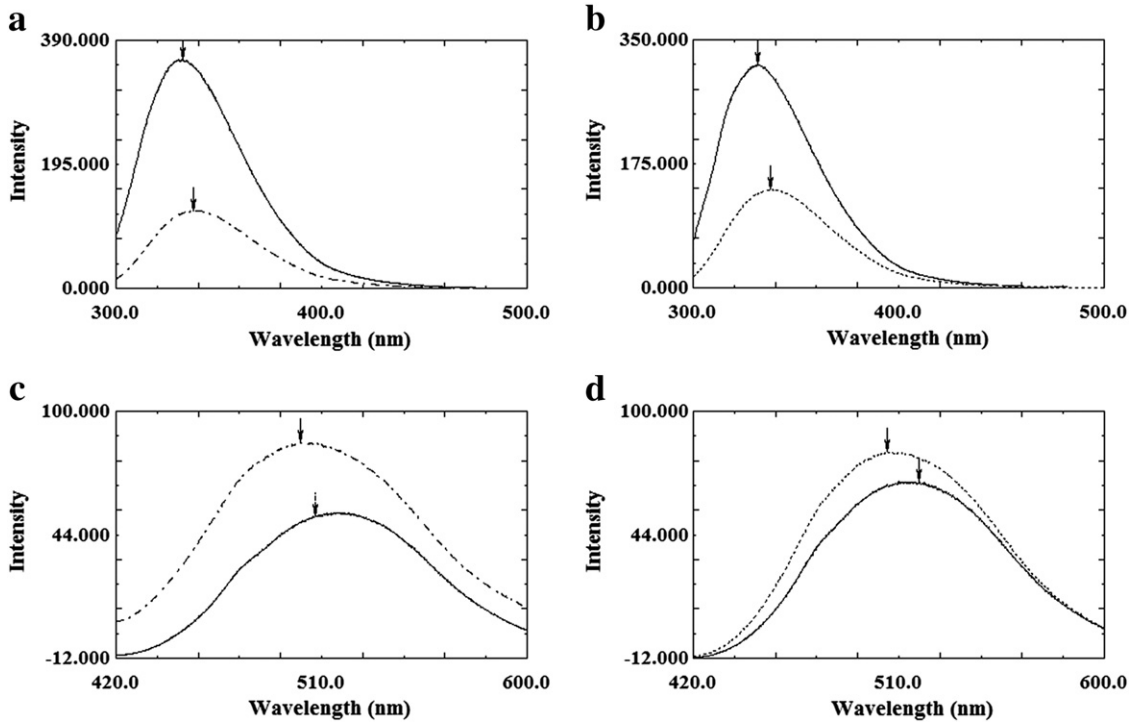

Fig. 5. Structural changes induced by binding of OA detected by intrinsic (a, b) and ANS-binding (c, d) fluorescence emission spectra. All spectra were measured at room temperature at a scan interval of 0.2 nm. A and C are spectra of LF samples while B and D are spectra of α-LA samples. Solid lines and dotted lines represent the spectra of control protein and protein–OA complexes, respectively. The arrow in each figure indicated the position of λ_{max}.

multiple pathways, and both the protein and OA contributed to the anti-tumor activity of protein–OA complexes.

The lipocalins are a family of proteins that can bind small hydrophobic molecules such as long chain fatty acids [59]. All members of this family contain a β-barrel shaped into a flattened calyx, which constitutes the internal binding cavity for small hydrophobic molecules [59]. The binding site for OA in α-LA was reported to be around the Ca^{2+}-binding cleft [21,22]. LF is composed of two globular lobes of similar size and 40% sequence identity [60]. Each lobe was folded into α-helical and β-sheet structures [20,61] and connected by a hinge region, which created a deep cleft for iron binding [62]. Therefore, it can be deduced that each lobe of LF could bind OA while there is only one lobe in α-LA that could bind OA. This was confirmed by the ITC results. The stoichiometry of OA in LF-OA was almost two-fold that in LA–OA.

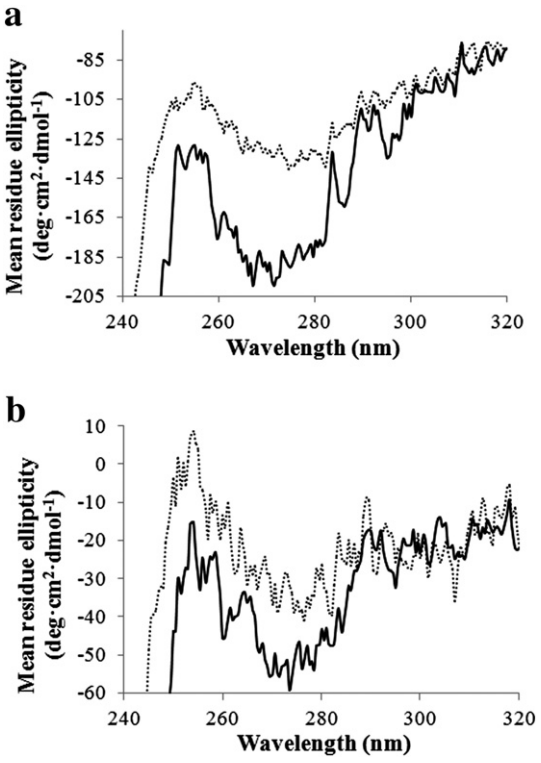

Fig. 6. Structural characteristics of LF–OA (a) and α-LA–OA (b) detected by near-UV CD spectra. All spectra were measured at room temperature at a scan interval of 50 nm/min. Each spectrum was averaged from three scans. Solid lines and dotted lines represent the spectra of control protein and protein–OA complexes, respectively.

Binding of OA resulted in the exposure of Trp to a more hydrophilic environment and increased the exposure of hydrophobic regions (Fig. 5). In addition, LF–OA showed a loss of tertiary structure compared with the control LF. These spectroscopic features are consistent with those of α-LA–OA [7–9,15,16,18,63]. The difference between LF–OA and α-LA–OA is the change of secondary structure content. LF–OA showed a decrease of α-helix and β-turn while in α-LA–OA the α-helix was unchanged and the β-turn decreased. However, both LF–OA and α-LA–OA showed an increase in β-sheet and random coil, which may explain the loss of tertiary structure.

All chemical, physical, and biological processes are accompanied by changes in thermodynamic parameters [36,37]. ΔG determines whether a reaction can take place spontaneously under certain conditions, while changes in ΔH and ΔS reflect the interaction forces. ΔH reflects the amount of heat released or absorbed during the course of the

Table 1
Secondary structure content calculated from the far-UV CD according to Yang's reference.

Content (%)	LF–OA	Control LF	LA–OA	Control α-LA
α-Helix	19.51 ± 0.52 *	25.13 ± 0.91	26.40 ± 0.25	26.07 ± 0.25
β-Sheet	36.70 ± 2.77 *	28.50 ± 0.89	20.36 ± 0.72 *	14.30 ± 0.66
β-Turn	12.45 ± 1.73 *	15.64 ± 0.35	17.00 ± 0.47 *	20.26 ± 0.31
Random	31.34 ± 0.46 *	30.73 ± 0.06	36.27 ± 0.45 *	39.37 ± 0.26

* Indicates $p < 0.05$.

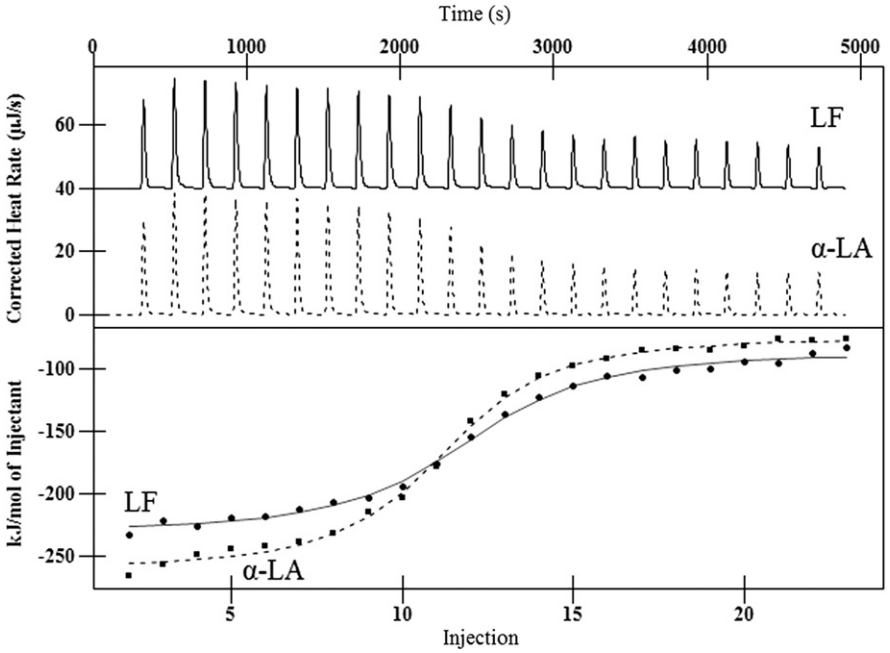

Fig. 7. Calorimetric titration (upper figure) and plots of the integrated heat versus each injection (lower figure) fit to an independent binding site model. 1.68 mM OA was titrated to 6.41 μM LF (solid lines) or 11.2 μM α-LA (dotted lines) at 45 °C with a stirring rate of 150 rpm/min. Both the proteins and OA were dissolved in 10 mM pH 8.0 PBS.

reaction [36,37,64] while ΔS reflects a change in the degree of order of the system, which is also influenced by changes in the conformation of the macromolecules and the restriction of degrees of freedom of the main chain and side groups of macromolecules [36,37]. The interaction between endogenous or exogenous ligands and biological macromolecules involves not only electrostatic interactions and hydrophobic interactions but also hydrogen bonds and van der Waals interactions [39,65]. Previous studies inferred that α-LA interacts with OA through hydrophobic [3,66] or electrostatic [67] interactions. In our study, the negative value of ΔH and ΔS during the binding reactions indicated that van der Waals forces and hydrogen bonds play a major role in OA binding to LF and α-LA [34,39,65,68].

In conclusion, LF can bind OA to form HAMLET-like complexes but with a much higher anti-tumor activity. LF–OA kills tumor cells by inducing apoptosis, which was initiated by both the mitochondria-mediated intrinsic pathway and death receptor-mediated extrinsic pathway. Besides its anti-tumor mechanism, the structural changes of LF induced by OA binding were also similar to those observed for the HAMLET-like complexes, including exposure of Trp residues and the hydrophobic clusters. Although the change of α-helix and β-turn content is different between LF and α-LA, both proteins showed increased content of β-sheet and random coil. LF exhibited a higher affinity to OA than to α-LA although both proteins interacted with OA through van der Waals interactions and hydrogen bonds. Although follow-up studies on the complexes are needed, the study revealed a novel anti-tumor HAMLET-like complex. This study provides the theoretical basis for exploration of proteins that acquire new biological activities after complex formation with small molecules such as fatty acids.

5. Conclusions

Questions have been raised as to whether anti-tumor complexes similar to HAMLET can be formed from other proteins. This study revealed that LF could also bind OA and induce apoptosis in tumor cells. Both LF and α-LA interact with OA through van der Waals forces and hydrogen bonds. LF–OA induced high anti-tumor activity through apoptosis initiated by both death-receptor and mitochondrial-mediated pathways. The binding capability of OA in LF was about twice that of OA in α-LA. Although it was reported that the anti-tumor activity of HAMLET depends on OA, our study found that both the protein and OA were responsible for the anti-tumor activity. Structural changes of LF induced by binding OA were similar to HAMLET, including the exposure of Trp residues and hydrophobic surface areas, loss of tertiary structure and increased content of β-sheet and random coil structures. Our study confirmed the presence of a novel HAMLET-like complex, while the comparison of LF–OA and α-LA–OA provides new information on the interactions between the proteins and OA, which provides a theoretical basis for further investigations.

Acknowledgements

We gratefully acknowledge the financial support from the Ministry of Science and Technology of China (2012BAD28B08), the International Science and Technology Cooperation Program of China (2011DFA32550), and the Beijing Municipal Commission of Education Co-constructed Program.

Table 2
ITC results.[a]

OA binding kinetics	n	K (M^{-1})	ΔH (kJ/mol)	ΔS (kJ/mol)[b]	ΔG (kJ/mol)[c]
LF	34.77 ± 0.30	(1.58 ± 0.83) × 10^5	−145.12 ± 10.63	−356.51 ± 21.7	−31.65 ± 1.87
α-LA	18.51 ± 0.10	(2.09 ± 1.39) × 10^5	−186.90 ± 12.49	−485.53 ± 30.9	−32.39 ± 2.22

[a] The reported thermodynamic parameters are apparent values and include the contributions to the overall equilibrium from fatty acid, protein and buffer species. The thermodynamic parameters n, K, and ΔH are obtained from the ITC fitting software, Launch NanoAnalyze 2.0.
[b] Calculated from ΔS = (ΔH − ΔG) / T.
[c] Calculated from ΔG = −RTlnK.

References

[1] M. Svensson, C. Düringer, O. Hallberg, A. Mossberg, A. Hakansson, S. Linse, C. Svanborg, HAMLET—a complex from human milk that induces apoptosis in tumor cells but spares healthy cells, Adv. Exp. Med. Biol. 503 (2002) 125–132.

[2] A. Håkansson, B. Zhivotovsky, S. Orrenius, H. Sabharwal, C. Svanborg, Apoptosis induced by a human milk protein, Proc. Natl. Acad. Sci. U. S. A. 92 (1995) 8064–8068.

[3] W. Fischer, L. Gustafsson, A.K. Mossberg, J. Gronli, S. Mork, R. Bjerkvig, C. Svanborg, Human alpha-lactalbumin made lethal to tumor cells (HAMLET) kills human glioblastoma cells in brain xenografts by an apoptosis-like mechanism and prolongs survival, Cancer Res. 64 (2004) 2105–2112.

[4] A.K. Mossberg, Y. Hou, M. Svensson, B. Holmqvist, C. Svanborg, HAMLET treatment delays bladder cancer development, J. Urol. 183 (2010) 1590–1597.

[5] L. Gustafsson, I. Leijonhufvud, A. Aronsson, A.K. Mossberg, C. Svanborg, Treatment of skin papillomas with topical alpha-lactalbumin-oleic acid, N. Engl. J. Med. 350 (2004) 2663–2672.

[6] A.K. Mossberg, B. Wullt, L. Gustafsson, W. Månsson, E. Ljunggren, C. Svanborg, Bladder cancers respond to intravesical instillation of HAMLET (human alpha-lactalbumin made lethal to tumor cells), Int. J. Cancer 121 (2007) 1352–1359.

[7] M. Svensson, A. Håkansson, A.K. Mossberg, S. Linse, C. Svanborg, Conversion of α-lactalbumin to a protein inducing apoptosis, Proc. Natl. Acad. Sci. U. S. A. 97 (2000) 4221–4226.

[8] T. Kamijima, A. Ohmura, T. Sato, K. Akimoto, M. Itabashi, M. Mizuguchi, M. Kamiya, T. Kikukawa, T. Aizawa, M. Takahashi, K. Kawano, M. Demura, Heat-treatment method for producing fatty acid-bound alpha-lactalbumin that induces tumor cell death, Biochem. Biophys. Res. Commun. 376 (2008) 211–214.

[9] E.L. Knyazeva, V.M. Grishchenko, R.S. Fadeev, V.S. Akatov, S.E. Permyakov, E.A. Permyakov, Who is Mr. HAMLET? Interaction of human α-lactalbumin with monomeric oleic acid, Biochemistry 47 (2008) 13127–13137.

[10] S.E. Permyakov, E.L. Knyazeva, M.V. Leonteva, R.S. Fadeev, A.V. Chekanov, A.P. Zhadan, A.P. Håkansson, V.S. Akatov, E.A. Permyakov, A novel method for preparation of HAMLET-like protein complexes, Biochimie 93 (2011) 1495–1501.

[11] M. Zhang, F. Yang Jr., F. Yang, J. Chen, C.Y. Zheng, Y. Liang, Cytotoxic aggregates of α-lactalbumin induced by unsaturated fatty acid induce apoptosis in tumor cells, Chem. Biol. Interact. 180 (2009) 131–142.

[12] B. Fang, M. Zhang, L. Jiang, H. Jing, F.Z. Ren, Influence of pH on the structure and oleic acid binding ability of bovine α-lactalbumin, Protein J. 31 (2012) 564–572.

[13] J. Pettersson, A.K. Mossberg, C. Svanborg, α-Lactalbumin species variation, HAMLET formation, and tumor cell death, Biochem. Biophys. Res. Commun. 345 (2006) 260–270.

[14] M.S. Atri, A.A. Saboury, A.A. Moosavi-Movahedi, B. Goliaei, Y. Sefidbakht, H.H. Alijanvand, A. Sharifzadeh, A. Niasari-Naslaji, Structure and stability analysis of cytotoxic complex of camel α-lactalbumin and unsaturated fatty acids produced at high temperature, J. Biomol. Struct. Dyn. 28 (2011) 919–928.

[15] S. Tolin, G. De Franceschi, B. Spolaore, E. Frare, M. Canton, P. Polverino de Laureto, A. Fontana, The oleic acid complexes of proteolytic fragments of alpha-lactalbumin display apoptotic activity, FEBS J. 277 (2010) 163–173.

[16] K. Wilhelm, A. Darinskas, W. Noppe, E. Duchardt, K.H. Mok, V. Vukojević, J. Schleucher, L.A. Morozova-Roche, Protein oligomerization induced by oleic acid at the solid–liquid interface—equine lysozyme cytotoxic complexes, FEBS J. 276 (2009) 3975–3989.

[18] K. Liš ková, M.A.E. Auty, V. Chaurin, S. Min, K.H. Mok, N. O'Brien, A.L. Kelly, A. Brodkorb, Cytotoxic complexes of sodium oleate with β-lactoglobulin, Eur. J. Lipid Sci. Technol. 113 (2011) 1207–1218.

[18] L. Adlerova, A. Bartoskova, M. Faldyna, Lactoferrin: a review, Vet. Med. Czech. 53 (2008) 457–468.

[19] L. Sánchez, M. Calvo, J.H. Brock, Biological role of lactoferrin, Arch. Dis. Child. 67 (1992) 657–661.

[20] J.H. Nuijens, P.H. van Berkel, F.L. Schanbacher, Structure and biological actions of lactoferrin, J. Mammary Gland Biol. Neoplasia 1 (1996) 285–295.

[21] A. Casbarra, L. Birolo, G. Infusini, F.D. Piaz, M. Svensson, P. Pucci, C. Svanborg, G. Marino, Conformational analysis of HAMLET, the folding variant of human α-lactalbumin associated with apoptosis, Protein Sci. 13 (2004) 1322–1330.

[22] J. Fast, A.K. Mossberg, H. Nilsson, C. Svanborg, M. Akke, S. Linse, Compact oleic acid in HAMLET, FEBS Lett. 579 (2005) 6095–6100.

[23] A. Ohashi, E. Murata, K. Yamamoto, E. Majima, E. Sano, Q.T. Le, N. Katunuma, New functions of lactoferrin and β-casein in mammalian milk as cysteine protease inhibitors, Biochem. Biophys. Res. Commun. 306 (2003) 98–103.

[24] G. Brisson, M. Britten, Y. Pouliot, Heat-induced aggregation of bovine lactoferrin at neutral pH: effect of iron saturation, Int. Dairy J. 17 (2007) 617–624.

[25] E.N. Baker, H.M. Baker, A structural framework for understanding the multifunctional character of lactoferrin, Biochimie 91 (2009) 3–10.

[26] D.L. Felicea, J. Sun, R.H. Liu, A modified methylene blue assay for accurate cell counting, J. Funct. Foods 1 (2009) 109–118.

[27] B. Fang, H.Y. Guo, M. Zhang, L. Jiang, F.Z. Ren, The six amino acid antimicrobial peptide bLFcin6 penetrates cells and delivers siRNA, FEBS J. 280 (2013) 1007–1017.

[28] B. Fang, L. Jiang, M. Zhang, F.Z. Ren, A novel cell-penetrating peptide TAT-A1 delivers siRNA into tumor cells selectively, Biochimie 95 (2013) 251–257.

[29] M.J. Cliff, A. Gutierrez, J.E. Ladbury, A survey of the year 2003 literature on applications of isothermal titration calorimetry, J. Mol. Recognit. 17 (2004) 513–523.

[30] A. Ababou, J.E. Ladbury, Survey of the year 2004: literature on applications of isothermal titration calorimetry, J. Mol. Recognit. 19 (2006) 79–89.

[31] A. Ababou, J.E. Ladbury, A survey of the year 2005 literature on applications of isothermal titration calorimetry, J. Mol. Recognit. 20 (2007) 4–14.

[32] O. Okhrimenkoa, I. Jelesarov, A survey of the year 2006 literature on applications of isothermal titration calorimetry, J. Mol. Recognit. 21 (2008) 1–19.

[33] Y. Liang, Applications of isothermal titration calorimetry in protein science, Acta Biochim. Biophys. Sin. (Shanghai) 40 (2008) 565–576.

[34] P.D. Ross, S. Subramanian, Thermodynamics of protein association reactions: forces contributing to stability, Biochemistry 20 (1981) 3096–3102.

[35] T.S. Singh, S. Mitra, Interaction of cinnamic acid derivatives with serum albumins: a fluorescence spectroscopic study, Spectrochim. Acta A 78 (2011) 942–948.

[36] A.R. Cestaria, E.F.S. Vieiraa, J.A. Simonib, C. Airoldi, Thermochemical investigation on the adsorption of some divalent cations on modified silicas obtained from sol–gel process, Thermochim. Acta 348 (2000) 25–31.

[37] P. Liu, Q.S. Wang, X. Li, C.C. Zhang, Zeta-potentials and enthalpy changes in the process of electrostatic self-assembly of cations on silica surface, Powder Technol. 193 (2009) 46–49.

[38] L. Ding, P.J. Zhou, S.Q. Li, G.Y. Shi, T. Zhong, M. Wu, Spectroscopic studies on the thermodynamics of L-cysteine capped CdSe/CdS quantum dots-BSA interactions, J. Fluoresc. 21 (2011) 17–24.

[39] M. De, C.C. You, S. Srivastava, V.M. Rotello, Biomimetic interactions of proteins with functionalized nanoparticles: a thermo dynamic study, J. Am. Chem. Soc. 129 (2007) 10747–10753.

[40] C.R. Brinkmann, C.W. Heegaard, T.E. Petersen, J.C. Jensenius, S. Thiel, The toxicity of bovine α-lactalbumin made lethal to tumor cells is highly dependent on oleic acid and induces killing in cancer cell lines and noncancer-derived primary cells, FEBS J. 278 (2011) 1955–1967.

[41] M. Wei, Y. Xu, Q. Zou, L. Tu, C. Tang, T. Xu, L. Deng, C. Wu, Hepatocellular carcinoma targeting effect of PEGylated liposomes modified with lactoferrin, Eur. J. Pharm. Sci. 46 (2012) 131–141.

[42] B.Y. Bi, B. Leveugle, J.L. Liu, A. Collard, P. Coppe, A.C. Roche, N. Nillesse, M. Capron, G. Spik, J. Mazurier, Immunolocalization of the lactotransferrin receptor on the human T lymphoblastic cell line Jurkat, Eur. J. Cell Biol. 65 (1994) 164–171.

[43] C. Garré, G. Bianchi-Scarra, M. Sirito, M. Musso, R. Ravazzolo, Lactoferrin binding sites and nuclear localization in K562 (s) cells, J. Cell. Physiol. 153 (1992) 477–482.

[44] B.Y. Bi, J.L. Liu, D. Legrand, A.C. Roche, M. Capron, G. Spik, J. Mazurier, Internalization of human lactotransferrin by the Jurkat human lymphoblastic T-cell line, Eur. J. Cell Biol. 69 (1995) 288–296.

[45] E. Rochard, D. Legrand, M. Lecocq, R. Hamelin, M. Crepin, J. Montreuil, G. Spik, Characterization of lactotransferrin receptor in epithelial cell lines from non-malignant human breast, benign mastopathies and breast carcinomas, Anticancer Res. 12 (1992) 2047–2052.

[46] D. Roiron-Lagroux, M. Amouric, J. Marvaldi, C. Figarella, Lactoferrin-binding sites at the surface of HT-29 D4 cells, Eur. J. Biochem. 186 (1989) 367–373.

[47] T. Mikogami, T. Marianne, G. Spik, Effect of intracellular iron depletion by picolinic acid on expression of the lacto-ferrin receptor in the human colon carcinoma cell subclone HT29-18-C1, Biochem. J. 308 (1995) 391–397.

[48] A. Kogan, N. Garti, Microemulsions as transdermal drug delivery vehicles, Adv. Colloid Interface Sci. 123–126 (2006) 369–385.

[49] S. Arur, U.E. Uche, K. Rezaul, M. Fong, V. Scranton, A.E. Cowan, W. Mohler, D.K. Han, Annexin I is an endogenous ligand that mediates apoptotic cell engulfment, Dev. Cell 4 (2003) 587–598.

[50] O. Hallgren, L. Gustafsson, H. Irjala, G. Selivanova, S. Orrenius, C. Svanborg, HAMLET triggers apoptosis but tumor cell death is independent of caspases, Bcl-2 and p53, Apoptosis 11 (2006) 221–233.

[51] I.M. Ghobrial, T.E. Witzig, A.A. Adjei, Targeting apoptosis pathways in cancer therapy, CA Cancer J. Clin. 55 (2005) 178–194.

[52] S. Elmore, Apoptosis: a review of programmed cell death, Toxicol. Pathol. 35 (2007) 495–516.

[53] Y. Kondoh, T. Kawada, R. Urade, Activation of caspase 3 in HepG2 cells by elaidic acid (t18:1), Biochim. Biophys. Acta 1771 (2007) 500–505.

[54] E. Kishida, M. Tajiri, Y. Masuzawa, Docosahexaenoic acid enrichment can reduce L929 cell necrosis induced by tumor necrosis factor, Biochim. Biophys. Acta 1761 (2006) 454–462.

[55] A. Nishiyama, C.R. Cavaglieri, R. Curi, P.C. Calder, Arachidonic acid-containing phosphatidylcholine inhibits lymphocyte proliferation and decreases interleukin-2 and interferon-Q production from concanavalin A-stimulated rat lymphocytes, Biochim. Biophys. Acta 1487 (2000) 50–60.

[56] C.P. Diggle, In vitro studies on the relationship between polyunsaturated fatty acids and cancer: tumour or tissue specific effects? Prog. Lipid Res. 41 (2002) 240–253.

[57] N. Guthrie, K.K. Carroll, Specific versus non-specific effects of dietary fat on carcinogenesis, Prog. Lipid Res. 38 (1999) 261–271.

[58] C.H. Jakobsen, G.L. Størvold, H. Bremseth, T. Follestad, K. Sand, M. Mack, K.S. Olsen, A.G. Lundemo, J.G. Iversen, H.E. Krokan, S.A. Schønberg, DHA induces ER stress and growth arrest in human colon cancer cells: associations with cholesterol and calcium homeostasis, J. Lipid Res. 49 (2008) 2089–2100.

[59] D.R. Flower, The lipocalin protein family: structure and function, Biochem. J. 318 (1996) 1–14.

[60] J.R. Lu, S. Perumal, X.B. Zhao, Surface-induced unfolding of human lactoferrin, Langmuir 21 (2005) 3354–3361.

[61] J.L. Gifford, H.N. Hunter, H.J. Vogel, Lactoferricin: a lactoferrin-derived peptide with antimicrobial, antiviral, antitumor and immunological properties, Cell. Mol. Life Sci. 62 (2005) 2588–2598.

[62] E.N. Baker, B.E. Anderson, H.M. Baker, C.L. Day, M. Haridas, G.E. Norris, S.V. Rumball, C.A. Smith, D.H. Thomas, Three-dimensional structure of lactoferrin in various functional states, Adv. Exp. Med. Biol. 357 (1994) 1–12.

[63] J. Fast, A.K. Mossberg, C. Svanborg, S. Linse, Stability of HAMLET-a kinetically trapped alpha-lactalbumin oleic acid complex, Protein Sci. 14 (2005) 329–340.

[64] J.R. Horn, D. Russell, E.A. Lewis, K.P. Murphy, Van't Hoff and calorimetric enthalpies from isothermal titration calorimetry: are there significant discrepancies? Biochemistry 40 (2001) 1774–1778.
[65] D. Leckband, Measuring the forces that control protein interactions, Annu. Rev. Biophys. Biomol. Struct. 29 (2000) 1–26.
[66] C. Barbana, M.D. Pérez, L. Sánchez, M. Dalgalarrondo, J.M. Chobert, T. Haertlé, M. Calvo, Interaction of bovine α-lactalbumin with fatty acids as determined by partition equilibrium and fluorescence spectroscopy, Int. Dairy J. 16 (2006) 18–25.
[67] Y. Xie, S. Min, N.P. Harte, H. Kirk, J.E. O'Brien, H.P. Voorheis, C. Svanborg, H.K. Mok, Electrostatic interactions play an essential role in the binding of oleic acid with α-lactalbumin in the HAMLET-like complex: a study using charge-specific chemical modifications, Proteins 81 (2013) 1–17.
[68] F. Bou-Abdallah, T.R. Terpstra, The thermodynamic and binding properties of the transferrins as studied by isothermal titration calorimetry, Biochim. Biophys. Acta 1820 (2012) 318–325.